Letters to the Editor

Bent Hysteresis and Its Realization

ROBERT W. NEWCOMB

Abstract—**Bent hysteresis, which is hysteresis that bends over before a jump, is mathematically developed and circuit realizations given. The ideas are applicable to the design of chaotic systems.**

I. Introduction

In an interesting paper Shinriki, Yamamoto, and Mori [1] have shown that a van der Pol oscillator constructed with a nonlinearity which we will call here "bent hysteresis," rather than cubic polynomial, exhibits some new phenomena. In particular with certain parameter ratios a random waveform resulted. Thus the system appears to be what is otherwise now called "chaotic" [2] [3]. Since this chaotic behavior has subsequently been verified [4], a study of the basic component, the bent hysteresis, seems in order. This is undertaken here. In particular describing equations are obtained and two electronic realizations are presented for voltage-controlled characteristics. The results are for dc behavior, that is "resistive hysteresis," though one could pursue dynamical properties through semistate theory [5]. As general background for ideas of this correspondence one can refer to Chua [6].

II. Bent Hysteresis Definition

In order to give a feeling for its nature, Fig. 1 shows several typical measured bent hysteresis curves. Clearly the input–output curves of Fig. 1 can be closely approximated by a piecewise linear curve and thus we use Fig. 2 to precisely define the concept. That is, given eight break point pairs (V_{i1}, V_{o1}) through (V_{i8}, V_{o8}) and two end slopes S_1 and S_8, by forming straight lines connected as in Fig. 2 a multivalued curve is obtained which we define to be idealized *bent hysteresis*. In actual fact it is primarily the portion between (V_{i2}, V_{o2}) through (V_{i7}, V_{o7}) which is of interest in cases such as that of [1] (where the remainder of the curves has been ignored). But, as seen in Fig. 1, other bends practically occur and hence we take them into account. We will also assume the input break points satisfy $V_{i1} \leqslant V_{i2} < V_{i7} \leqslant V_{i8}$ while allowing various orderings of the remaining V_i's (though always falling between V_{i1} and V_{i8} and with $V_{i3} \leqslant V_{i6}$, $V_{i4} \leqslant V_{i6}$ and $V_{i3} \leqslant V_{i5}$). Fig. 2 defines what we may call "direct" bent hysteresis while by taking its negative (i.e., reflecting in the v_o axis) we get an "inverted" bent hysteresis.

III. Resistor Realization

Although we shall later modify the results to obtain v_o versus v_i curves, as per Fig. 1, we begin by considering a series connection of two piecewise linear resistors, one being positive and the other negative near the origin. And because of the possible use of active circuits we take the origin as possibly off of the curves, even

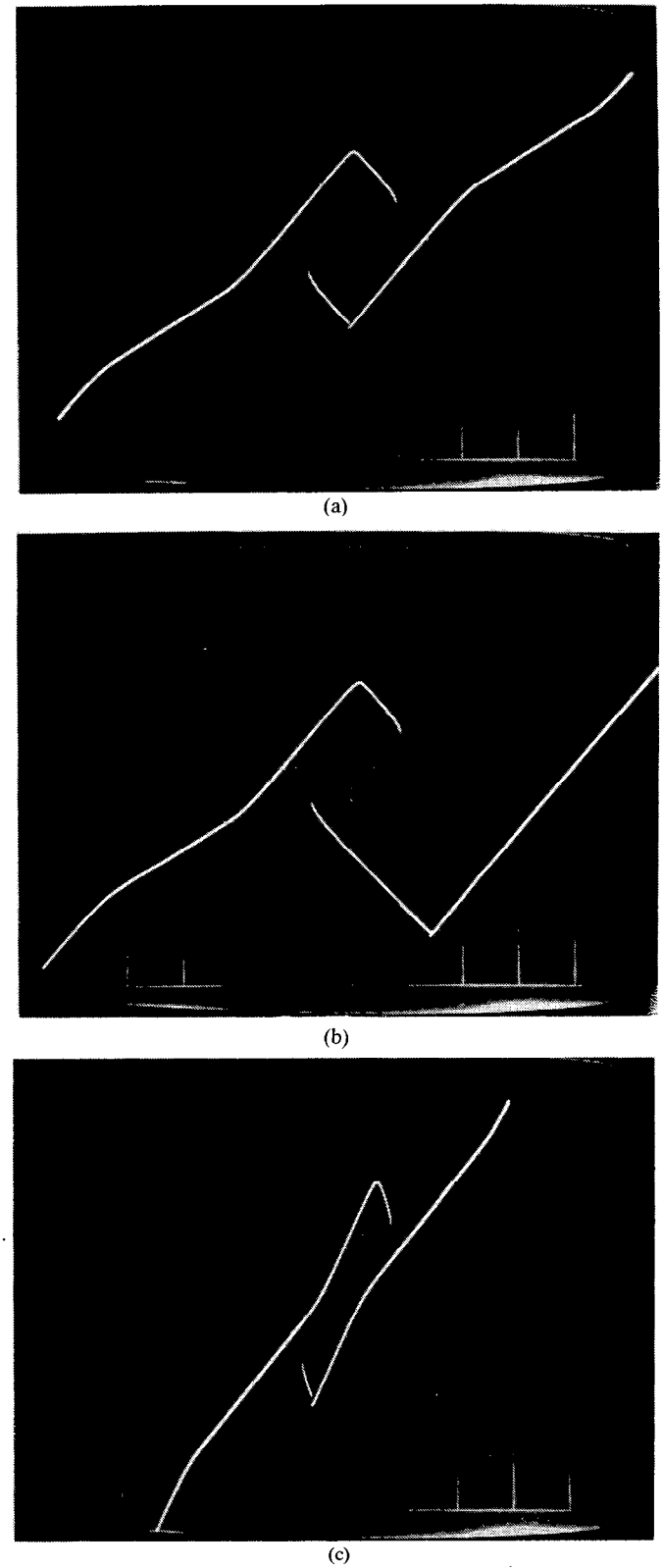

Fig. 1. Typical measured bent hysteresis curves: v_i, Horizontal, 0.5 V/div; v_o, Vertical, 1 V/div for (a) and (b), 0.5 V/div for (c); $f = 10$ Hz.

Manuscript received August 28, 1981; revised February 4, 1982. This work is based on work supported in part by the National Science Foundation under Grant ECS-8105507 and in part under the Microsystems and Generalized Networks Program with Z. Aziz subassistance.

The author is with Microsystems Laboratory, Electrical Engineering Department, College Park, MD 20742.

0098-4094/82/0700-0478$00.75

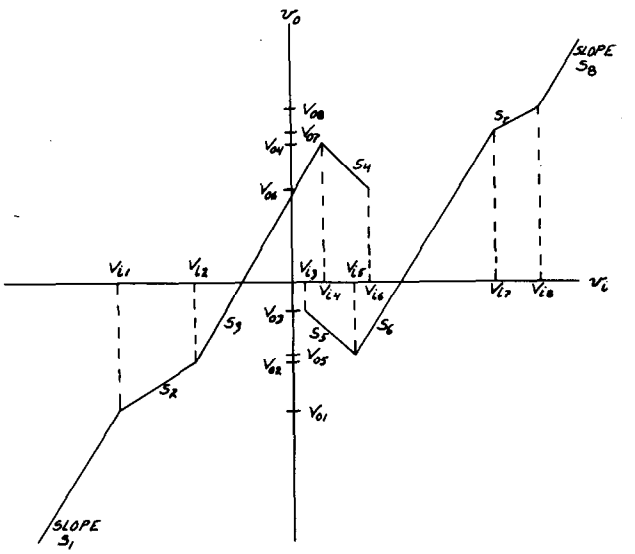

Fig. 2. Piecewise linear bent hysteresis, defining break points.

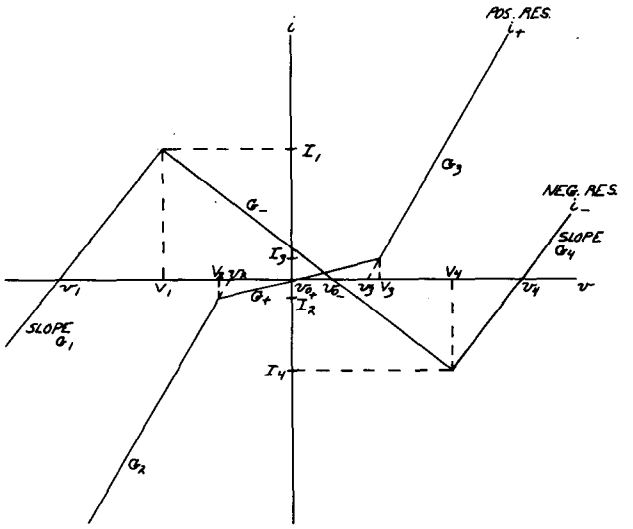

Fig. 3. Piecewise resistors, defining break points.

though by a normalization it could be taken at their intersection. Using voltage-controlled resistors Fig. 3 shows the two separate resistor curves while again defining the break points (V_1, I_1) through (V_4, I_4) and (conductance) slopes G_-, G_+, G_1 through G_4 (G_- negative, and the others nonnegative) as well as voltage axis intercepts v_1 through v_4 and (offsets) v_{o-}, v_{o+}. Thus the equations for the two curves are

$$\text{Neg. Res. } i_- = \begin{cases} G_1(v - v_1), & v \leq V_1 & \text{(1a)} \\ G_-(v - v_{o-}), & V_1 \leq v \leq V_4,\ G_- < 0 & \text{(1b)} \\ G_4(v - v_4), & V_4 \leq v & \text{(1c)} \end{cases}$$

$$\text{Pos. Res. } i_+ = \begin{cases} G_2(v - v_2), & v \leq V_2 & \text{(2a)} \\ G_+(v - v_{o+}), & V_2 \leq v \leq V_3 & \text{(2b)} \\ G_3(v - v_3), & V_3 \leq v. & \text{(2c)} \end{cases}$$

These two equations serve to define the two current functions of v, $i_-(v)$, and $i_+(v)$. Typical measured curves are shown in Fig.

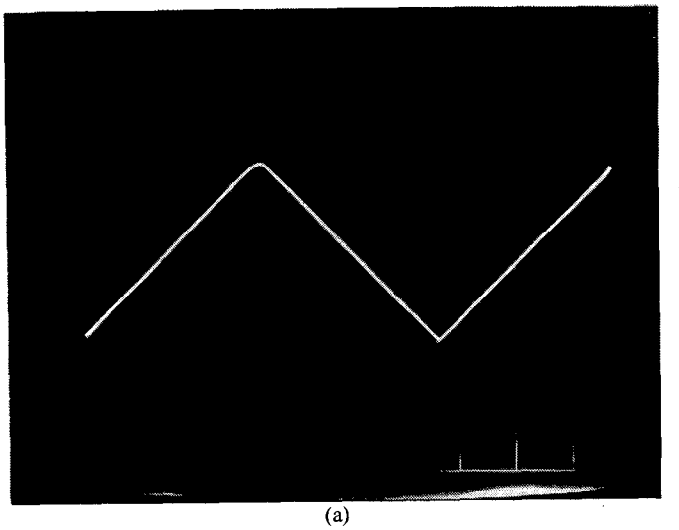

(a)

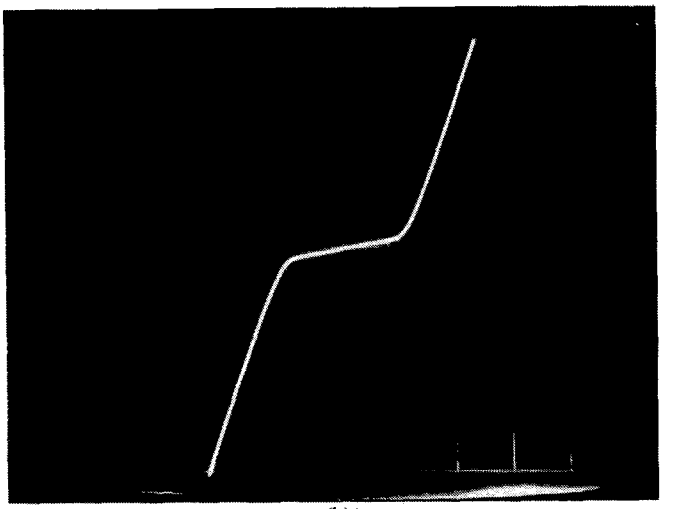

(b)

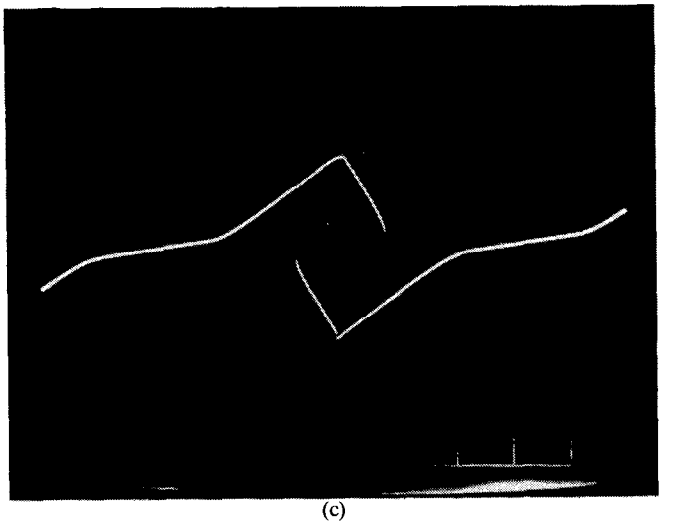

(c)

Fig. 4. Measured curves v, Horizontal, 0.5 V/div; i, Vertical, 50 μA/div; (a) i_- versus v_-. (b) i_+ versus v_+. (c) $i = i_- = i_+$ versus $v = v_+ + v_-$.

4(a) and (b), these being those used to obtain Fig. 1(a).

Placing the two resistors in series gives bent hysteresis, Fig. 4(c) showing a typical case for the resistors of Fig. 4(a) and (b). The resulting curve of $i(v)$ can be calculated by using the connection

laws

$$i_+(v_+)=i_-(v_-)=i(v) \tag{3a}$$

and

$$v=v_+ + v_-. \tag{3b}$$

That is, v_+ and v_- are solved for using (3a) which also determines the composite i, while the series voltage is the sum of the component voltages via (3b). Since our curves are assumed to be piecewise linear the calculations of (3) are simple though there are a number of them, as (1) and (2) give $3^2=9$ different equations (3a) to which must be added $9-1=8$ for determination of the break points of the composite curve (this being of the form of Fig. 2).

IV. Conversion to v_o versus v_i

In order to convert the $i-v$ bent hysteresis characteristic obtained from the last section to a v_o-v_i characteristic, consider the op-amp configuration of Fig. 5 where $i=f(v)$ is the bent hysteresis of Section III. If we assume that the op-amp is biased such that it operates in its nonsaturation region, then the describing equations are

$$v_i=v \tag{4a}$$

and

$$v_o=v+R_L i=v_i+R_L f(v_i). \tag{4b}$$

Thus the resistive bent hysteresis characteristic becomes scaled by the load resistance R_L and linearly shifted. Using results obtained for $i=f(v)$ the describing equations of this v_o-v_i bent hysteresis are

Upper Branch:

$$v_o=\begin{cases} v_i+\dfrac{R_L}{R_1+R_2}[v_i-(v_1+v_2)], & v_i\le V_{\mathrm{I}} \\ v_i+\dfrac{R_L}{R_1+R_+}[v_i-(v_1+v_{o+})], & V_{\mathrm{I}}\le v_i\le V_{\mathrm{II}} \\ v_i+\dfrac{R_L}{R_1+R_3}[v_i-(v_1+v_3)], & V_{\mathrm{II}}\le v_i\le V_{\mathrm{IV}} \\ v_i+\dfrac{R_L}{R_-+R_3}[v_i-(v_3+v_{o-})], & V_{\mathrm{IV}}\le v_i\le V_{\mathrm{VI}} \end{cases} \tag{5U}$$

Lower Branch:

$$v_o=\begin{cases} v_i+\dfrac{R_L}{R_2+R_-}[v_i-(v_2+v_{o-})], & V_{\mathrm{III}}\le v_i\le V_{\mathrm{V}} \\ v_i+\dfrac{R_L}{R_2+R_4}[v_i-(v_2+v_4)], & V_{\mathrm{V}}\le v_i\le V_{\mathrm{VIII}} \\ v_i+\dfrac{R_L}{R_4+R_+}[v_i-(v_4+v_{o+})], & V_{\mathrm{VII}}\le v_i\le V_{\mathrm{VIII}} \\ v_i+\dfrac{R_L}{R_3+R_4}[v_i-(v_3+v_4)], & V_{\mathrm{VIII}}\le v_i. \end{cases} \tag{5L}$$

The break points are readily calculated and are presented in Table I. As can be seen there are 16 equalities to be satisfied but only 12 parameters (G_1-G_4, G_+, G_-, V_1-V_4, v_{o+}, and v_{o-}) from which it is clear that arbitrary specifications of bent hysteresis break points are not realizable by the circuit of Fig. 5. However, usually one is not concerned about realizing (V_{i1}, V_{o1}), (V_{i2}, V_{o2}), (V_{i7}, V_{o7}), and (V_{i8}, V_{o8}), while v_{o+} and v_{o-} are not usually free parameters, in which case there are eight equations and 10 unknowns. Thus there is a good possibility of realizing desirable bent hysteresis characteristics with the circuit of Fig. 5.

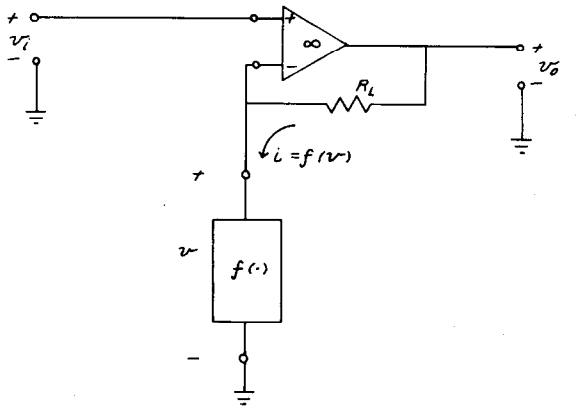

Fig. 5. Conversion of $i(v)$ to $v_o(v_i)$ bent hysteresis

TABLE I
Bent Hysteresis Break Point Equations v_o-v_i Form

$V_{i1} = (1-G_-R_1)V_1+(1+G_+R_1)V_2-G_+R_1v_{o+}+G_-R_1v_{o-}$
$V_{o1} = V_{i1}+R_LI_2,\ I_2=G_+(V_2-v_{o+})$

$V_{i2} = (1-G_-R_1)V_1+(1+G_+R_1)V_3-G_+R_1v_{o+}+G_-R_1v_{o-}$
$V_{o2} = V_{i2}+R_LI_3,\ I_3=G_+(V_3-v_{o+})$

$V_{i3} = (1+G_+R_-)V_2-G_+R_-v_{o+}+v_{o-}$
$V_{o3} = V_{i3}+R_LI_2,\ I_2=G_+(V_2-v_{o+})$

$V_{i4} = (1+G_-R_3)V_1+(1-G_+R_3)V_3+G_+R_3v_{o+}-G_-R_3v_{o-}$
$V_{o4} = V_{i4}+R_LI_1,\ I_1=G_-(V_1-v_{o-})$

$V_{i5} = (1-G_+R_2)V_2+(1+G_-R_2)V_4+G_+R_2v_{o+}-G_-R_2v_{o-}$
$V_{o5} = V_{i5}+R_LI_4,\ I_4=G_-(V_4-v_{o-})$

$V_{i6} = (1+G_+R_-)V_3-G_+R_-v_{o+}+v_{o-}$
$V_{o6} = V_{i6}+R_LI_3,\ I_3=G_+(V_3-v_{o+})$

$V_{i7} = (1+G_+R_4)V_2+(1-G_-R_4)V_4-G_+R_4v_{o+}+G_-R_4v_{o-}$
$V_{o7} = V_{i7}+R_LI_2,\ I_2=G_+(V_2-v_{o+})$

$V_{i8} = (1+G_+R_4)V_3+(1-G_-R_4)V_4-G_+R_4v_{o+}+G_-R_4v_{o-}$
$V_{o8} = V_{i8}+R_LI_3,\ I_3=G_+(V_2-v_{o+})$

V. Circuit Realizations

A number of circuit configurations are available for realization of the bent hysteresis characteristics so far discussed. Basic to most of these circuits are negative resistor realizations, that of [7, p. 15] being used here. By placing a linear resistor in series or parallel with the negative resistor, resistors with positive slope

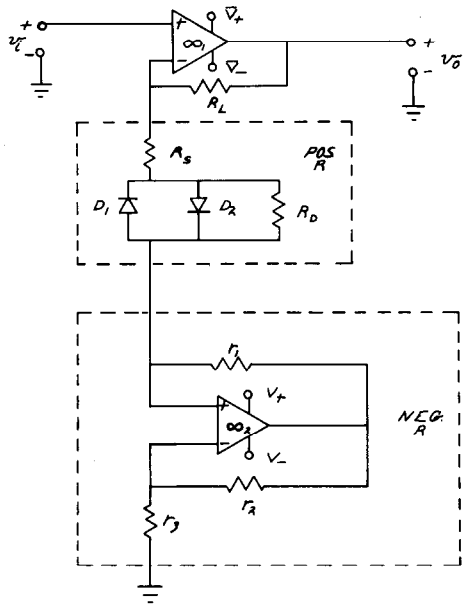

Fig. 6. Grounded $i(v)$ and v_o versus v_i bent hysteresis circuit. Circuit used for Fig. 1 with op-amp's = MC1458 $V_+ = 7 = -V_-$, $V_+ = 2.5$, $V_- = -3.8$, $R_L = 20$ kΩ, $R_s = 3$ kΩ, $r_1 = r_2 = r_3 = 10$ kΩ, $D_1 = D_2 = 2N4123$ n-p-n transistors connected as diodes, $R_D = 56$ kΩ.

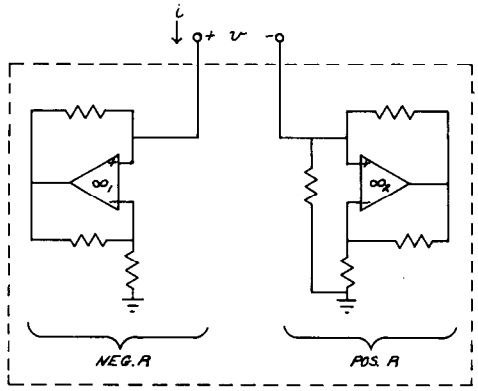

Fig. 7. Floating $i(v)$ bent hysteresis circuit.

and the same break points can be obtained. Using these components and possibly diodes we can electronically realize bent hysteresis.

A. First Realization — Grounded $i(v)$ and v_o versus v_i Forms

In order to make a series connection of a broken-slope positive resistor with the negative voltage-controlled resistor of [7, p. 15] the positive resistor can be constructed of diodes, as suggested by the circuit in [1]. The number of back-back diodes controls the break point voltages $V_2 = -V_3$, as multiples of $0.5v$ if silicon junction diodes are used (or $0.2v$ if Schottky diodes are used). This connection gives $v_{o+} = 0$ and yields a small G_+ and large $G_2 = G_3$; controlled but larger G_+ and smaller $G_2 = G_3$ can be obtained by adding resistors in parallel and series. The combination of a diode realized positive resistor and an op-amp realized negative resistor placed in series when used, as per Fig. 5, yields a v_o versus v_i bent hysteresis characteristic of the type developed in the previous sections.

Fig. 6 shows a particular configuration with numerical values chosen to give Fig. 1a). Back-back diodes give $V_3 = -V_2 \approx 0.5v$, $v_{o+} = v_{o-} = 0$ while we choose $G_L R_+ = 2.5$, $G_L R_- = -0.5$, $G_L R_2 = G_L R_3 = 3/14$, $V_4 = -V_1 = 0.8$, $R_1 = R_4 = -R_-$ with R_S and R_D chosen to give $(V_{i4}, V_{o4}) = (-V_{i5}, -V_{o5}) = (0, 1.6)$ and $(V_{i6}, V_{o6}) = (-V_{i3}, -V_{o3}) = (0.4, 0.6)$.

The other two traces of Fig. 1 were obtained from Fig. 6 by changing the negative resistor op-amp's bias with the other components fixed as for Fig. 1(a) ($V_+ = 4.4v$, $V_- = -3.8v$ for Fig. 1(b), and $V_+ = 1.4v$, $V_- = -3v$ for Fig. 1(c)).

Amplification can occur before the input and after the output of Fig. 6 to obtain scaled versions of a realized bent hysteresis, thus making the circuit of Fig. 6 relatively versatile.

B. Second Realization — Floating $i(v)$ Form

Due to the reason that resistors realized by the circuit of [7, p. 15] practically require one terminal grounded, their simultaneous use is most convenient in situations where another one-port can be connected between their upper terminals, as illustrated in Fig. 7. When such a possibility exists, this gives one of the most exact realizations of the $i = f(v)$ form of bent hysteresis. It is,

however, more difficult to check experimentally. Nevertheless, the availability of simple and independent adjustment of the break points, via resistor ratios or op-amp bias voltages, makes the circuit of Fig. 7 extremely attractive.

VI. Discussion

Here we have shown that a given bent hysteresis curve can be conveniently realized by electronic circuits, at least over reasonable ranges of the parameters. Experimentation has proven the validity of the results as well as the robustness of the resulting circuits. The theory and results presented are for the static characteristics of bent hysteresis, the experimental curves, as Fig. 1, holding for frequencies below several hundred hertz.

As can be seen there are some constraints on designs possible; for example, $V_{o6} \geq V_{i6}$ since $V_{o6} = V_{i6} + R_L I_3$. Consequently it is of interest to develop design equations. Likewise the circuits are for voltage controlled devices and, thus the development of current-controlled bent hysteresis circuits would be of interest.

References

[1] M. Shinriki, M. Yamamoto, and S. Mori, "Multimode oscillations in a modified van der Pol oscillator containing a positive nonlinear conductance," *Proc. IEEE*, vol. 69, pp. 394–395, Mar. 1981.

[2] Y. Ueda and N. Akamatsu, "Chaotically transistional phenomena in the forced negative-resistance oscillator," *IEEE Trans. Circuits Syst.*, vol. CAS-28, pp. 217–224, Mar. 1981.

[3] J. Guckenheimer, "Dynamics of the van der Pol equation," *IEEE Trans. Circuits Syst.*, vol. CAS-27, pp. 983–989, Nov. 1980.

[4] D. Elliot, "Multimode oscillations in a van der Pol oscillator containing a positive nonlinear conductance", Report for ENEE 418, Univ. of Maryland, June 1981.

[5] R. W. Newcomb, "Semistate design theory: Binary and swept hysteresis," *Circuits, Systems, and Signal Processing*, to appear.

[6] L. O. Chua, *Introduction to Nonlinear Network Theory*. New York: McGraw-Hill, 1969.

[7] T. Endo and S. Mori, "Mode analysis of a ring of a large number of mutually coupled van der Pol oscillators," *IEEE Trans. Circuits and Systems*, vol. CAS-25, pp. 7–18, Jan. 1978.

Approximation of 2-D Weakly Causal Filters

BIJAN LASHGARI AND LEONARD M. SILVERMAN

***Abstract*—A technique for approximating 2-D weakly causal filters by recursive ones is presented which also includes the design of nonsymmetric half-plane (NSHP) filters. An example is given to illustrate the proposed technique.**

I. Introduction

In this paper we consider the problem of approximating 2-D weakly causal filters. This class, as defined by Eising [2], includes the nonsymmetric half-plane (NSHP) filters [14] considered by many authors [5]–[8] in 2-D estimation and spectral analysis. The algorithm we present is a generalization of a method we recently introduced [1] for approximation of quarter-plane causal filters. This generalization is facilitated by making use of the mapping technique such as the one reported in [2], [11], [12]. Particularly, we adopt the formulation in [2] since it is compatible with the state-space approach we present here. The algorithm is then applied to an example used in the recent paper [4] and it is shown that a considerably better approximation is obtained.

Manuscript received April 28, 1981; revised November 9, 1981 and January 11, 1982. This work was supported in part by the U.S. Army Research under Grant DAAG29-79-C-0054 and the National Science Foundation under Grant ECS-8011911.

The authors are with the Department of Electrical Engineering, University of Southern California, Los Angeles, CA 90007.

II. Approximation Algorithm

We will first review several of the definitions given in [2].

Definition (2.1): The *support* of the 2-D impulse response matrix $H_{i,j} \in \mathbb{R}^{s \times w}$ is defined as the set

$$S_H = \{(i,j) | (i,j) \in Z^2, H_{i,j} \neq 0\}$$

where Z denotes the set of integers, $\mathbb{R}$ denotes the field of real numbers, and $\mathbb{R}^{s \times w}$ denotes the set of s by w matrices with real elements.

Definition (2.2): A *cone* C is a subset of $\mathbb{R}^2$ such that if $(x,y) \in C$ then $(\lambda x, \lambda y) \in C$ for all $\lambda \geq 0$.

Note that $(x,y) \in (-C)$ if and only if $(-x,-y) \in C$.

Definition (2.3): A *causality cone* $C_{p,r|q,t}$ is a cone defined by the intersection of two half planes $P_{p,r}$ and $P_{q,t}$, where

$$P_{p,r} = \{(x,y) | (x,y) \in \mathbb{R}^2, px + ry \geq 0\}$$

$$P_{q,t} = \{(x,y) | (x,y) \in \mathbb{R}^2, qx + ty \geq 0\}$$

and p, r, q, and t are nonnegative integers satisfying $pt - qr = 1$.

Note that $C_{p,r|q,t} \cap (-C_{p,r|q,t}) = \{(0,0)\}$ and $Q_1 \subset C_{p,r|q,t}$ (Q_1 denotes the first quadrant of $\mathbb{R}^2$).

Definition (2.4): The 2-D impulse response matrix $H_{i,j} \in \mathbb{R}^{s \times w}$, $(i,j) \in Z^2$, is said to be *weakly causal* with causality cone $C_{p,r|q,t}$ if there exists a cone C such that

$$C \cap (-C) = \{(0,0)\}, \qquad Q_1 \subset C$$

and

$$S_H \subset C \subset C_{p,r|q,t}$$

where S_H is the support of $H_{i,j}$

Suppose now $H_{i,j} \in \mathbb{R}^{s \times w}$ is a 2-D weakly causal impulse response matrix with causality cone $C_{p,r|q,t}$ (Definition (2.4)). We consider the problem of approximating $H_{i,j}$ in such a way that the approximation has the same causality cone but can be implemented with a lower order filter. The approach for approximation of this class of 2-D filters is to find an invertible transformation to move the data into the first quadrant without moving the origin. Then after performing the approximation outlined in [1] on the data in the transformed domain the resultant approximation will be transferred back to the original coordinates. The approximation result obtained in the transformed domain (first quadrant) is a causal, recursive, and separable in denominator (CRSD) filter [1] which has the advantage of simple implementation (because of recursiveness) and stability test (because of separability of the denominator [9], [10]). In addition, the invertibility of the transformation permits the stability test and other analysis to be carried out equivalently in the transformed domain. Thus all the benefits of the technique in [1] for the quarter-plane causal filters can be extended to the 2-D weakly causal ones with this approach.

The next theorem identifies such an invertible transformation.

Theorem (2.1) [2]: Let $C_{p,r|q,t}$ be the causality cone associated with a weakly causal impulse response $H_{i,j} \in \mathbb{R}^{s \times w}$, $(i,j) \in S_H$, then the transformation

$$\phi: C_{p,r|q,t} \to Q_1$$

0098-4094/82/0700-0482$00.75 ©1982 IEEE